Journal of Molecular Liquids 171 (2012) 11–15

Contents lists available at SciVerse ScienceDirect

Journal of Molecular Liquids

journal homepage: www.elsevier.com/locate/molliq

Role of tautomerism and solvatochromism in UV–VIS spectra of arylhydrazones of β-diketones

Wojciech Kuznik [a], Maximilian N. Kopylovich [b], Gunel I. Amanullayeva [c], Armando J.L. Pombeiro [b,]*, Ali H. Reshak [d,e], Kamran T. Mahmudov [b], I.V. Kityk [a,f,]**

[a] Department of Physical Chemistry and Polymer Technology, Silesian University of Technology, Gliwice, Poland
[b] Centro de Química Estrutural, Complexo I, Instituto Superior Técnico, TU Lisbon, Av. Rovisco Pais, 1049-001 Lisbon, Portugal
[c] Institute of Petrochemical Processes, National Academy of Sciences of Azerbaijan, Hojaly Ave. 30, 1025 Baku, Azerbaijan
[d] School of Complex Systems, FFWP, University of South Bohemia, Nove Hrady 37333, Czech Republic
[e] School of Material Engineering, Malaysia University of Perlis, P.O. Box 77, d/a Pejabat Pos Besar, 01007 Kangar, Perlis, Malaysia
[f] Electrical Engineering Department, Czestochowa University of Technology, Av. Armii Krajowej 17/19, PL-42200 Czestochowa, Poland

ARTICLE INFO

Article history:
Received 8 September 2011
Received in revised form 21 March 2012
Accepted 23 March 2012
Available online 9 April 2012

Keywords:
Arylhydrazones of β-diketones
Tautomeric equilibrium
Solvatochromism

ABSTRACT

New arylhydrazones of β-diketones, 5-chloro-3-(2-(1-ethoxy-1,3-dioxobutan-2-ylidene)hydrazinyl)-2-hydroxybenzenesulfonic acid (**1**), 3-(2-(1-ethoxy-1,3-dioxobutan-2-ylidene)hydrazinyl)-2-hydroxy-5-nitrobenzenesulfonic acid (**2**), and 3-(2-(4,4-dimethyl-2,6-dioxocyclohexylidene) hydrazinyl)-2-hydroxy-5-nitrobenzenesulfonic acid (**3**), have been synthesized and characterized by IR, ^{1}H and ^{13}C NMR spectroscopies and elemental analysis. **3** and known 5-(2-(4,4-dimethyl-2,6-dioxocyclohexylidene)hydrazinyl)-4-hydroxybenzene-1,3-disulfonic acid (**4**) exist in DMSO solution exclusively in the hydrazone form, while **1** and **2** exist in DMSO and H_2O solutions as a mixture of enol-azo and hydrazone tautomeric forms, in ratios dependent on the solvent polarity and inductive effect of the substituents. DFT and TDDFT approaches were applied for simulations of experimental UV–VIS absorption spectra of the studied compounds, taking into account solvatochromic as well as tautomeric effect. The performed simulations have established a correlation of substantial experimental 120 nm red shift of the enol-azo form with respect to hydrazone with HOMO and LUMO orbitals' delocalization.

1. Introduction

Arylhydrazones of β-diketones (AHBD, Scheme 1) are compounds extensively studied due to their prototropic tautomerism and strong intramolecular resonance-assisted hydrogen bonds (RAHB) [1–5], which are similar to those formed within the widely used β-diketones [6,7]. The mentioned RAHB system can play a principal role for the application of AHBD e.g. as bistate molecular switches [8–11]. The equilibrium between enol-azo ⇌ hydrazone tautomeric forms is dependent on several factors determined by the molecular structure of AHBD and external factors (e.g. solvent, temperature) [1]. It was established that in AHBD formed by asymmetric β-diketones a six-membered H-bonded ring is generated at the more sterically favorable side of the molecule [1,12,13]. Moreover, usually in solid phase all the structurally studied AHBD are stabilized in the hydazone form [1,3,10,14–16], while in solution the investigated unsymmetrical AHBD exist as a mixture of enol-azo and hydrazone tautomers (Scheme 1) [1].

On the other hand, study of the solvatochromic properties of AHBD demonstrated that they can be applied for qualitative analysis of aprotic solvents in protic ones [16]. Upon dissolution the intermolecular hydrogen and van-der-Waals interactions with the solvent molecules change the partial distribution of the tautomers. Sometimes the presence of both tautomeric forms can hamper the interpretation of the spectroscopic data due to the bands overlapping [1], while theoretical calculations allow one to overcome these difficulties by rationalizing the relation between the tautomeric ratio and properties [1,3,17].

The principal goals of this work are as follows: *i*) to synthesize new AHBD, namely 5-chloro-3-(2-(1-ethoxy-1,3-dioxobutan-2-ylidene) hydrazinyl)-2-hydroxybenzenesulfonic acid (**1**), 3-(2-(1-ethoxy-1,3-dioxobutan-2-ylidene)hydrazinyl)-2-hydroxy-5-nitrobenzenesulfonic acid (**2**), and 3-(2-(4,4-dimethyl-2,6-dioxocyclohexylidene)hydrazinyl)-2-hydroxy-5-nitrobenzenesulfonic acid (**3**) (Scheme 1); *ii*) to trace the influence of the introduced substituents on the tautomeric balance and the physico-chemical properties of AHBD as well as their known analog 5-(2-(4,4-dimethyl-2,6-dioxocyclohexylidene)hydrazinyl)-4-hydroxybenzene-1,3-disulfonic acid (**4**) [5]; *iii*) to present a detailed

---

* Corresponding author. Fax: +351 218464455.
** Correspondence to: I.V. Kityk, Electrical Engineering Department, Czestochowa University of Technology, Av. Armii Krajowej 17/19, PL-42200 Czestochowa, Poland. Fax: +48 34 3250 821.
E-mail addresses: pombeiro@ist.utl.pt (A.J.L. Pombeiro), iwank74@gmail.com (I.V. Kityk).

0167-7322/$ – see front matter. Crown Copyright © 2012 Published by Elsevier B.V. All rights reserved.
doi:10.1016/j.molliq.2012.03.023

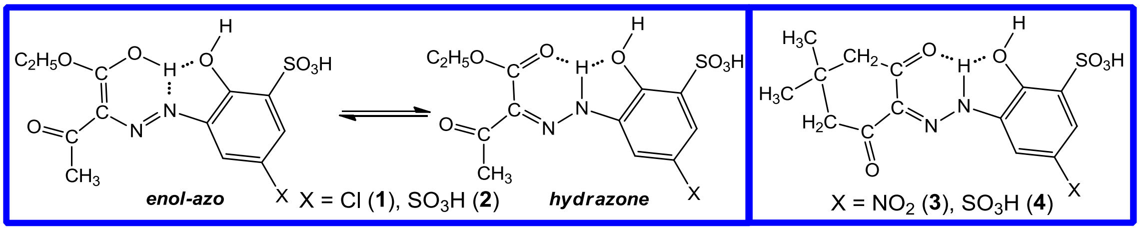

Scheme 1. Arylhydrazones of β-diketones considered in this work (both the enol-azo and hydrazone forms are presented).

procedure to simulate UV–VIS spectra of these compounds performing theoretical simulation at the DFT level, taking into account both solvatochromic and tautomeric effects. The tautomeric equilibrium of azo chromophores can lead to significant changes in absorption spectra. We attempt to explain this observed shift by delocalization of LUMO orbital and hence change in the excitation energy of the first excited state.

2. Experimental section

2.1. Materials and methods

The ^{1}H and ^{13}C NMR spectra were recorded at an ambient temperature on a Bruker Avance II + 300 (UltraShield™ Magnet) spectrometer operating at 300.130 and 75.468 MHz for proton and carbon-13, respectively. The chemical shifts are reported in ppm using tetramethylsilane (TMS) as an internal reference. The infrared spectra (4000–400 cm^{-1}) were recorded on a BIO-RAD FTS 3000MX instrument in KBr pellets. All the UV–VIS spectra were recorded with HP 8453 spectrophotometer in distilled water with a spectral resolution of 1 nm. Quartz cells with a light path of 1 cm were used.

2.2. Synthesis of the arylhydrazones of β-diketones

The studied compounds were prepared via the Japp–Klingemann reaction [18] involving diazotization of aromatic amines following azocoupling of thus formed diazonium salt and β-diketones in water solution containing sodium acetate [12,13].

2.2.1. Diazotization

A 0.025 mol portion of 3-amino-2-hydroxy-5-(substituted) benzenesulfonic acid was dissolved in 50 mL of water and then 1.00 g (0.025 mol) of crystalline NaOH was added. The solution was cooled in an ice bath to 273 K and then 1.725 g (0.025 mol) of $NaNO_2$ was added; after that 5.00 mL (33%) HCl was added in portions for 1 h. The temperature of the mixture should not exceed 278 K. The resulting diazonium solution was used directly in the following coupling procedure.

2.2.2. Azocoupling

8.20 g (0.100 mol) of CH_3COONa was added to a mixture of 0.025 mol of β-diketone with 100 mL of ethanol. The solution was cooled in an ice bath to ca. 273 K, and a suspension of 2-hydroxy-3-sulfo-5-(substituted)aryldiazonium chloride (see above) was added in three portions under vigorous stirring for 1 h.

The identity of **1–3** was demonstrated by element analysis, IR and ^{1}H and ^{13}C NMR spectrometry.

1: yield: 65% (based on 1-ethoxybutane-1,3-dione), yellow powder soluble in methanol, ethanol, water and insoluble in benzene and chloroform. Anal. Calcd for $C_{12}H_{13}ClN_2O_7S$ ($M = 364.76$): C, 39.51; H, 3.59; N, 7.68. Found: C, 39.37; H, 3.34; N, 7.52. IR (KBr, selected bands, cm^{-1}): 3678 ν(OH), 3065 ν(NH), 1745 ν(C═O), 1627 ν(C═O···H), 1541 ν(C═N). ^{1}H NMR of a mixture of tautomeric enol-azo and hydrazone forms (300.13 MHz, D_2O). Enol-azo, δ: 0.38–0.44 (3H, CH_3), 2.45 (3H, CH_3), 4.32–4.35 (2H, CH_2), 7.36–7.53 (2H, Ar–H). Hydrazone, δ: 1.33–1.37 (3H, CH_3), 2.34 (3H, CH_3), 4.32–4.35 (2H, CH_2), 7.36–7.53 (2H, Ar–H). ^{1}H NMR of a mixture of tautomeric enol-azo and hydrazone forms (300.13 MHz, DMSO-d_6). Enol-azo, δ: 1.25–1.28 (3H, CH_3), 2.42 (3H, CH_3), 4.26–4.29 (2H, CH_2), 7.18–7.48 (2H, Ar–H), 11.19 (1H, Ar–OH), 12.35 (1H, HO-enol). Hydrazone, δ: 1.30–1.33 (3H, CH_3), CH_3 signals were overlapped with the solvent peak, 4.31–4.33 (2H, CH_2), 7.18–7.48 (2H, Ar–H), 11.19 (1H, Ar–OH), 14.41 (1H, NH). ^{13}C{^{1}H} NMR (75.468 MHz, DMSO-d_6). Enol-azo, δ: 14.0 (CH_3), 26.8 (CH_3), 61.2 (CH_2), 114.4 (C–N), 114.7 (Ar–N═N), 122.8 (Ar–Cl), 127.3 and 132.7 (Ar–H), 133.5 (Ar–SO_3H), 141.9 (Ar–OH), 162.4 (C–O), 193.5 (C═O). Hydrazone, δ: 14.2 (CH_3), 30.6 (CH_3), 60.7 (CH_2), 117.6 and 121.1 (Ar–H), 122.0 (C═N), 129.0 (Ar–Cl), 131.3 (Ar–NH–N), 132.4 (Ar–SO_3H), 141.3 (Ar–OH), 164.1 and 196.4 (C═O).

2: yield: 62% (based on 1-ethoxybutane-1,3-dione), yellow powder soluble in methanol, ethanol, and water and insoluble in benzene and chloroform. Anal. Calcd for $C_{12}H_{14}N_2O_{10}S_2$ ($M = 410.38$): C, 35.12; H, 3.44; N, 6.83. Found: C, 35.06; H, 3.37; N, 6.76. IR (KBr, selected bands, cm^{-1}): 3516 ν(OH), 3043 ν(NH), 1737 ν(C═O), 1629 ν(C═O···H), 1548 ν(C═N). ^{1}H NMR of a mixture of tautomeric enol-azo and hydrazone forms (300.13 MHz, D_2O). Enol-azo, δ: 0.43–0.49 (3H, CH_3), 2.56 (3H, CH_3), 4.38–4.40 (2H, CH_2), 7.84–8.12 (2H, Ar–H). Hydrazone, δ: 1.33–1.38 (3H, CH_3), 2.39 (3H, CH_3), 4.38–4.40 (2H, CH_2), 7.84–8.12 (2H, Ar–H). ^{1}H NMR of a mixture of tautomeric enol-azo and hydrazone forms (300.13 MHz, DMSO-d_6). Enol-azo, δ: 1.27–1.30 (3H, CH_3), 2.41 (3H, CH_3), 4.27–4.29 (2H, CH_2), 7.58–7.84 (2H, Ar–H), 11.35 (1H, Ar–OH), 12.52 (1H, HO-enol). Hydrazone, δ: 1.27–1.30 (3H, CH_3), CH_3 signals were overlapped with the solvent peak, 4.31–4.33 (2H, CH_2), 7.58–7.84 (2H, Ar–H), 11.39 (1H, Ar–OH), 14.66 (1H, NH). ^{13}C{^{1}H} NMR (75.468 MHz, DMSO-d_6). Enol-azo, δ: 14.0 (CH_3), 26.6 (CH_3), 61.0 (CH_2), 112.5 (C–N), 113.2 (Ar–N═N), 126.7 (Ar–H), 128.7 (Ar–SO_3H), 130.0 (Ar–H), 139.6 (Ar–SO_3H), 142.5 (Ar–OH), 162.7 (C–O), 193.2 (C═O). Hydrazone, δ: 14.3 (CH_3), 30.6 (CH_3), 60.5 (CH_2), 120.1 and 121.0 (Ar–H), 128.1 (C═N), 128.6 (Ar–NH–N), 130.0 and 139.7 (Ar–SO_3H), 142.1 (Ar–OH), 164.3 and 196.2 (C═O).

3: yield: 87% (based on 5,5-dimethylcyclohexane-1,3-dione), yellow powder soluble in methanol, ethanol, water and insoluble in benzene and chloroform. Anal. Calcd for $C_{14}H_{15}N_3O_8S$ ($M = 385.35$): C, 43.64; H, 3.92; N, 10.90. Found: C, 43.45; H, 4.79; N, 10.74. IR (KBr, selected bands, cm^{-1}): 3620 ν(OH), 2960 ν(NH), 1688 ν(C═O), 1632 ν(C═O···H), 1592 ν(C═N). ^{1}H NMR (300.13 MHz, DMSO-d_6), δ: 1.03 (6H, 2CH_3), 2.39 (3H, CH_3), 2.60 (2H, CH_2), 2.69 (2H, CH_2), 8.12–8.35 (2H, Ar–H), 10.49 (1H, Ar–OH), 14.91 (1H, NH). ^{13}C{^{1}H} NMR (75.468 MHz, DMSO-d_6), δ: 28.0 (CH_3), 30.4 (CH_3), 38.7 (C_{ipso}), 51.9 (CH_2), 52.0 (CH_2), 110.9 and 118.9 (Ar–H), 130.6 (Ar–NH–N), 131.4 (Ar–SO_3H), 131.8 (C═N), 140.0 (Ar–NO_2), 148.1 (Ar–OH), 193.0 and 198.2 (C═O).

2.3. Computational procedure

All the DFT calculations were performed using GAUSSIAN09 package [19]. GABEDIT 2.3.6 Graphical User Interface [20] was used to generate input files and to depict graphs from output files. The calculations were performed at 6-31G (d,p) DFT B3LYP level with

PCM (Polarizable Continuum Model) [21,22] taking into account the external environment and simulated solvatochromism. Time-dependent density functional theory (TD-DFT) was used to simulate UV–VIS absorption spectra. Default geometry optimization algorithms converge to hydrazone form; to enforce enol-azo geometry Modredundant option was used and the OH bond was frozen during the calculation at length optimized in Molecular Mechanics run.

3. Results and discussion

3.1. Synthesis of **1**–**3** and spectroscopic study

New hydrazone compounds **1**–**3** and known [5] analog **4** were prepared by reaction of the β-diketones with the corresponding aryldiazonium chloride in the presence of sodium acetate. Compounds **1** and **2**, prepared from asymmetric β-diketone (1-ethoxybutane-1,3-dione), exist in D_2O and DMSO-d_6 solutions as mixtures of enol-azo and hydrazone tautomers (Scheme 1). The mole fraction of each tautomeric form has been determined by relative integration of the methyl (or methylene) group (Fig. 1) of each tautomer as reported [1]. With increase in the polarity of solvents (DMSO<D_2O) and the inductive effect of substituents ($-Cl < -SO_3H$, compare **1** and **2**) the tautomeric balance shifts to the enol-azo form (38% hydrazone, 62% enol-azo in DMSO and 14% hydrazone, 86% enol-azo in D_2O for **1**, and 13% hydrazone, 87% enol-azo in DMSO and 5% hydrazone, 95% enol-azo in D_2O for **2**). Nevertheless **1** and **2** were proved to exist in solution as a mixture of two tautomeric forms, IR spectrum (ν(NH) and ν(C=N) vibrations at 3065 and 3043, and 1541 and 1548 cm^{-1}, respectively) shows that in the solid state they are stabilized in the hydrazone form (Scheme 1) similarly to the reported analog [1]. In contrast, prepared from symmetrical 5,5-dimethylcyclohexane-1,3-dione compounds **3** and **4** are stabilized in both the mentioned solvents exclusively in the hydrazone form. It should be noted that the obtained data may be useful for some analytical applications [5,16] which require the knowledge of the distribution of the tautomers in a particular solvent.

3.2. Comparison of experimental and theoretical UV–VIS spectra

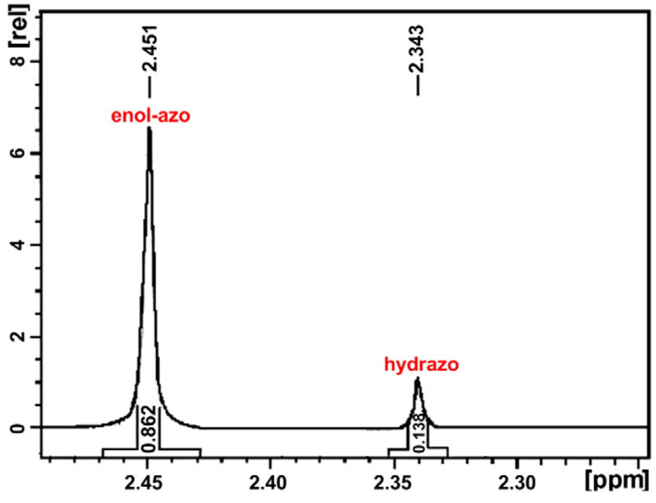

Fig. 1. Determination of the tautomeric ratio for **1** in D_2O ^1H NMR (see text).

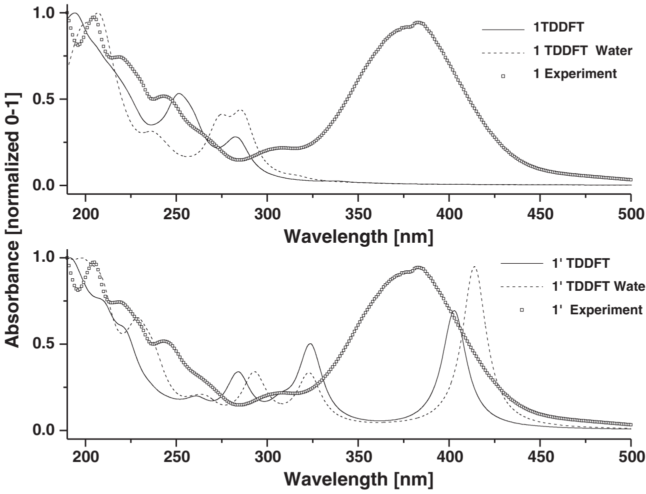

Fig. 2. Comparison of theoretically simulated and experimental UV–VIS spectra of **1** (top panel) and **1′** (bottom).

The experimental and theoretically simulated UV–VIS absorption spectra are presented in Figs. 2–5. In all the graphs experimental data are indicated by rectangles and theoretical predictions are indicated by solid (TDDFT without PCM) or dashed (TDDFT with PCM model compensating for water influence) lines. Spectra obtained for hydrazone forms of the studied compounds are given in top panels, while enol-azo forms are in bottom panels. In the case of **3** and **4** DFT simulations of both tautomers demonstrate similar absorption spectra (Figs. 4 and 5). According to NMR data these compounds exist in hydrazone form, however our simulations show that for **4** both forms have virtually identical absorption spectra, meaning that the results for **1** and **2** show significant difference for hydrazone and enol-azo forms. The TDDFT simulation for hydrazone tautomers indicates the first absorption peak in the spectral range of 250–280 nm. This is in evident contradiction with experimental data — the first absorption peak has a spectral maximum at approximately 370 nm. The enol-azo tautomers, on the other hand, were predicted to absorb light in the vicinity of 400 nm (no solvation model used) or 430 nm (PCM-simulated water influence). The reason for this considerable (up to 150 nm) red spectral shift between the hydrazone and enol-azo forms is the longer conjugated and orbital delocalized state of the latter both for HOMO and LUMO orbitals (Fig. 6), whereas for **3** and **4** tautomeric reaction does not result in significant change in orbital shape (Fig. 6). For the first chromophore these orbitals are localized in the carbonyl group, while for the latter they are both spread throughout the aromatic ring, including the hydroxyl substituent which is lying in one plane with the ring and the azo group. However, these tautomers do not differ significantly in atomic positions, different bond conjugations shift orbital energies significantly (Table 1). The NMR spectra confirm that the enol-azo

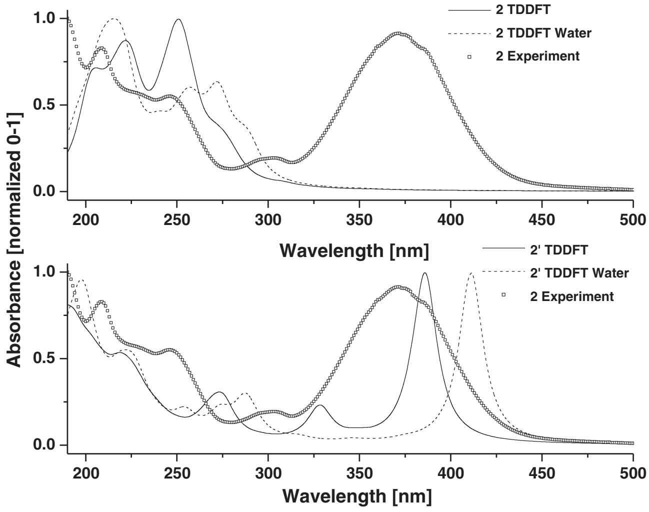

Fig. 3. Comparison of theoretically simulated and experimental UV–VIS spectra of **2** (top panel) and **2′** (bottom).

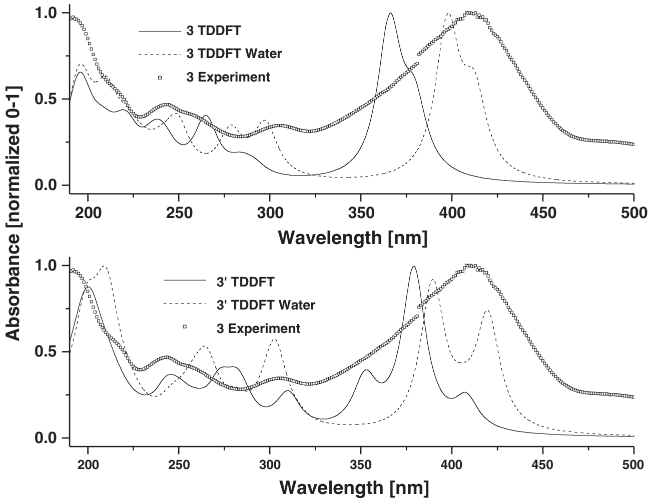

Fig. 4. Comparison of theoretically simulated and experimental UV–VIS spectra of **3** (top panel) and **3′** (bottom).

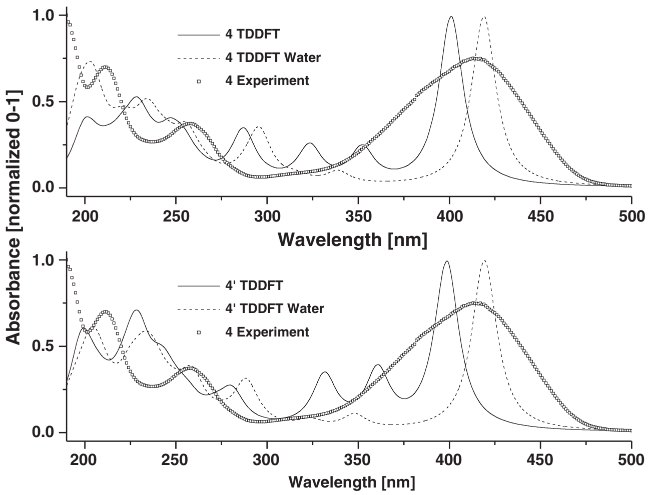

Fig. 5. Comparison of theoretically simulated and experimental UV–VIS spectra of **4** (top panel) and **4′** (bottom).

tautomer is dominant in both **1** and **2** following the conclusion from the TDDFT predicted absorption spectra. It is reasonable to assume that the tautomeric ratio is similar in D_2O used in the NMR experiment and H_2O used in the UV–VIS absorption measurement.

4. Conclusions

New AHBD (**1**–**3**) chromophores are synthesized and characterized. **1** and **2** exist in D_2O and DMSO-d_6 solutions as mixtures of enol-azo and hydrazone tautomers with predominance of the enol-azo form. The amount of enol-azo form depends on the substituent in the aromatic part of AHBD and solvent polarity, especially when this tautomer has longer conjugation length than the hydrazone one. TDDFT analysis of absorption spectra was validated with experimental data measured in water. DFT simulations of UV–VIS spectra of the studied compounds are confirmed by the NMR results, indicating a substantial red spectral shift of the enol-azo tautomer in the case for two of the studied compounds. Analysis of the theoretical simulations allows concluding that the significant (150 nm) spectral red shift between hydrazone and enol-azo tautomers originated from HOMO and LUMO orbital delocalization in the latter, which is obviously more important for compounds **1** and **2** with respect to **3** and **4**. It is principal that following the performed simulations at this level of theory hydrazone tautomers are the most stable in all the cases, regardless whether or not PCM solvation model was implemented for the calculations. Setting the enol group to freeze during the optimization algorithm was used in this study to enforce convergence to enol-azo geometry. Taking into account that presented AHBD compounds can exist in a number of tautomeric forms and their different conformations the results presented hereby are in satisfactory agreement with the UV–VIS experimental data.

Acknowledgments

This work has been partially supported by the Foundation for Science and Technology (FCT), Portugal, and its PPCDT (FEDER funded) and “Science 2007” programs. M.N.K. and K.T.M. express gratitude to the FCT for a working contract and a post-doc fellowship. The authors gratefully acknowledge the Portuguese NMR Network (IST-UTL Center) for the NMR facility.

Calculations have been carried out in Wroclaw Centre for Networking and Supercomputing (http://www.wcss.wroc.pl), grant no. 135.

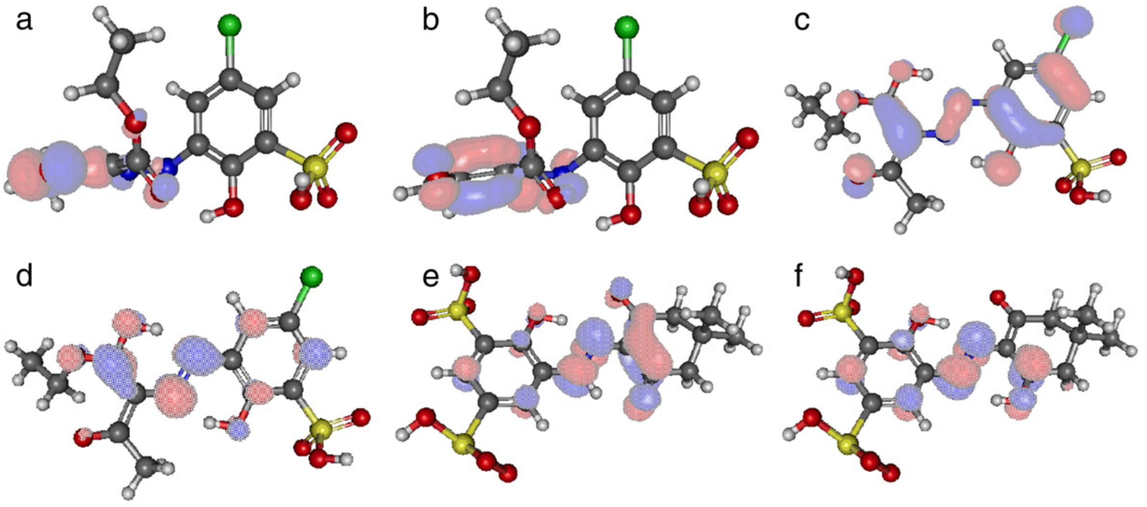

Fig. 6. 1 hydrazone form optimized in water (PCM) — HOMO (a)–LUMO (b) orbital; **1′** enol-azo form optimized in water (PCM) — HOMO (c)–LUMO (d) orbital; **4** hydrazone (e) and **4′** enol-azo (f) form optimized in water (PCM) — LUMO orbital.

Table 1
HOMO and LUMO orbital energies of the studied compounds, tautomeric forms and solvent influence simulated by PCM are presented (**1′–4′** represent the enol-azo form of compounds **1–4**).

eV	1	1′	2	2′	3	3′	4	4′
HOMO	−5.91	−5.36	−5.80	−5.85	−5.19	−5.14	−5.49	−5.41
LUMO	−3.16	−3.33	−3.14	−3.69	−3.38	−3.42	−3.56	−3.53
HOMO (water)	−5.63	−5.24	−5.47	−5.52	−5.65	−5.23	−5.46	−5.43
LUMO (water)	−2.72	−3.14	−2.75	−3.32	−3.40	−3.33	−3.38	−3.38

For author Ali H. Reshak the work was supported by the program RDI of the Czech Republic, the project CENAKVA (No. CZ.1.05/2.1.00/01.0024), and grant no. 152/2010/Z from the Grant Agency of the University of South Bohemia. Ali H. Reshak also acknowledges the School of Material Engineering, Malaysia University of Perlis, P.O. Box 77, d/a Pejabat Pos Besar, 01007 Kangar, Perlis, Malaysia.

References

[1] M.N. Kopylovich, K.T. Mahmudov, M.F.C.G. da Silva, M.L. Kuznetsov, P.J. Figiel, Y.Y. Karabach, K.V. Luzyanin, A.J.L. Pombeiro, Inorganic Chemistry 50 (2011) 918.
[2] K.T. Mahmudov, R.A. Rahimov, M.B. Babanly, P.Q. Hasanov, F.G. Pashaev, A.G. Gasanov, M.N. Kopylovich, A.J.L. Pombeiro, Journal of Molecular Liquids 162 (2011) 84.
[3] J. Marten, W. Seichter, E. Weber, U. Bohme, Journal of Physical Organic Chemistry 20 (2007) 716.
[4] M.N. Kopylovich, A.C.C. Nunes, K.T. Mahmudov, M. Haukka, T.C.O. Mac Leod, L.M.D.R.S. Martins, M.L. Kuznetsov, A.J.L. Pombeiro, Dalton Transactions 40 (2011) 2822.
[5] K.T. Mahmudov, A.M. Maharramov, R.A. Aliyeva, I.A. Aliyev, M.N. Kopylovich, A.J.L. Pombeiro, Analytical Letters 43 (2010) 2923.
[6] G. Aromi, P. Gamez, J. Reedijk, Coordination Chemistry Reviews 252 (2008) 964.
[7] P.A. Vigato, V. Peruzzo, S. Tamburini, Coordination Chemistry Reviews 253 (2009) 1099.
[8] P. Gilli, L. Pretto, V. Bertolasi, G. Gilli, Accounts of Chemical Research 42 (2009) 33.
[9] V. Bertolasi, V. Ferretti, P. Gilli, G. Gilli, Y.M. Issa, O.E. Sherif, Journal of the Chemical Society, Perkin Transactions 2 (1993) 2223.
[10] V. Bertolasi, P. Gilli, V. Ferretti, G. Gilli, K. Vaughan, New Journal of Chemistry 23 (1999) 1261.
[11] P. Gilli, V. Bertolasi, L. Pretto, A. Lycka, G. Gilli, Journal of the American Chemical Society 124 (2002) 13554.
[12] H.C. Yao, P. Resnick, Journal of the American Chemical Society 84 (1962) 3514.
[13] H.C. Yao, Journal of Organic Chemistry 29 (1964) 2959.
[14] J. Marten, W. Seichter, E. Weber, U. Bohme, CrystEngComm 10 (2008) 541.
[15] A.M. Maharramov, R.A. Aliyeva, I.A. Aliyev, F.G. Pashaev, A.G. Gasanov, S.I. Azimova, R.K. Askerov, A.V. Kurbanov, K.T. Mahmudov, Dyes and Pigments 85 (2010) 1.
[16] K.T. Mahmudov, A.M. Maharramov, R.A. Aliyeva, I.A. Aliyev, R.K. Askerov, R. Batmaz, M.N. Kopylovich, A.J.L. Pombeiro, Journal of Photochemistry and Photobiology A: Chemistry 219 (2011) 159.
[17] W. Kuznik, I.V. Kityk, M.N. Kopylovich, K.T. Mahmudov, K. Ozga, G. Lakshminarayana, A.J.L. Pombeiro, Spectrochimica Acta Part A: Molecular and Biomolecular Spectroscopy 78 (2011) 1287.
[18] F.R. Japp, F. Klingemann, Liebigs Annalen der Chemie 247 (1888) 190.
[19] M.J. Frisch, G.W. Trucks, H.B. Schlegel, G.E. Scuseria, M.A. Robb, J.R. Cheeseman, G. Scalmani, V. Barone, B. Mennucci, G.A. Petersson, H. Nakatsuji, M. Caricato, X. Li, H.P. Hratchian, A.F. Izmaylov, J. Bloino, G. Zheng, J.L. Sonnenberg, M. Hada, M. Ehara, K. Toyota, R. Fukuda, J. Hasegawa, M. Ishida, T. Nakajima, Y. Honda, O. Kitao, H. Nakai, T. Vreven, J.A. Montgomery Jr., J.E. Peralta, F. Ogliaro, M. Bearpark, J.J. Heyd, E. Brothers, K.N. Kudin, V.N. Staroverov, R. Kobayashi, J. Normand, K. Raghavachari, A. Rendell, J.C. Burant, S.S. Iyengar, J. Tomasi, M. Cossi, N. Rega, J.M. Millam, M. Klene, J.E. Knox, J.B. Cross, V. Bakken, C. Adamo, J. Jaramillo, R. Gomperts, R.E. Stratmann, O. Yazyev, A.J. Austin, R. Cammi, C. Pomelli, J.W. Ochterski, R.L. Martin, K. Morokuma, V.G. Zakrzewski, G.A. Voth, P. Salvador, J.J. Dannenberg, S. Dapprich, A.D. Daniels, O. Farkas, J.B. Foresman, J.V. Ortiz, J. Cioslowski, D.J. Fox, Gaussian 09, Revision A.02, Gaussian, Inc., Wallingford CT, 2009.
[20] A.R. Allouche, Journal of Computational Chemistry 32 (2011) 174.
[21] S. Miertus, E. Scrocco, J. Tomasi, Chemical Physics 55 (1981) 117.
[22] S. Miertus, J. Tomasi, Chemical Physics 65 (1982) 239.